Metamorphism, geochemistry and origin of magnesian volcanic rocks, Klamath Mountains, California

B. R. HACKER AND W. G. ERNST
Department of Geology, School of Earth Sciences, Stanford University, Stanford, CA 94305–2115, USA

M. D. BARTON*
Department of Earth and Space Sciences, University of California, Los Angeles, CA 90024–1567, USA

ABSTRACT Metabasaltic rocks in the Klamath Mountains of California with 'komatiitic' major element concentrations were investigated in order to elucidate the origin of the magnesian signature. Trace-element concentrations preserve relict igneous trends and suggest that the rocks are not komatiitic basalts, but immature arc rocks and within-plate alkalic lavas. Correlation of 'excess' MgO with the volume per cent hornblende (±clinopyroxene) suggests that the presence of cumulus phases contributes to the MgO-rich compositions. Early submarine alteration produced regional $\delta^{18}O$ values of $+10 \pm 1.5$‰ and shifts in Al_2O_3, Na_2O, and K_2O concentrations. Regional metamorphic grade in the study area varies from biotite-zone greenschist facies (350–550° C, *c.* 3 kbar) southward to prehnite–actinolite facies (200–400° C, ≤3 kbar), but little isotopic or elemental change occurred during the regional recrystallization. The greenschist facies assemblage is actinolitic hornblende + phengite + epidote + sodic plagioclase + microcline + chlorite + titanite + hematite + quartz in Ti-poor metabasaltic rocks; in addition to these phases biotite is present in Ti-rich analogues. Lower grade greenstones contain prehnite and more nearly stoichiometric actinolite. The moderate to low pressures of regional metamorphism are compatible with *P–T* conditions in a magmatic arc. Later contact metamorphism at 2–2.9 ± 0.5 kbar and at peak temperatures approaching 600° C around the English Peak and Russian Peak granodiorites produced 3–4-km-wide aureoles typified by gradual, systematic increases in the pargasite content of amphibole, muscovite content of potassic white mica, and anorthite content of plagioclase compositions. Metasomatism during contact metamorphism produced further increases in bulk-rock $\delta^{18}O_{SMOW}$ of as much as +6‰. Thus, the unusually MgO-rich nature of the Sawyers Bar rocks may be attributed at least partly to metasomatism and the presence of magnesian cumulus phases.

Key words: Klamath Mountains; komatiitic basalt; metasomatism; oxygen isotopes.

INTRODUCTION AND REGIONAL GEOLOGY

Ernst (1987) reported that polymetamorphosed Permian to Jurassic(?) mafic volcanic rocks (greenstones) in the Sawyers Bar area of the Klamath Mountains, California (Fig. 1), are compositionally similar to komatiitic basalts. Phanerozoic komatiitic basalts are unusual, and their occurrence in the Klamath Mountains might be of special tectonic significance, so an investigation was initiated to determine whether the highly magnesian compositions were the result of primary igneous processes, metamorphism, or some combination of the two. Moreover, the distinctive composition might be a powerful basis for correlating or differentiating these rocks from those of nearby terranes, if it could be shown that the composition was not related to some local secondary phenomenon such as post-accretion contact metamorphism. This paper reports the results of our investigation of the post-magmatic recrystallization textures and compositions, and discusses how metamorphic changes can be stripped away to reveal original igneous bulk-rock compositions. A companion paper (Ernst *et al.*, 1991) describes the igneous petrogenesis of these rocks. A third report (Ernst, 1990) deals with regional terrane analysis.

The Klamath Mountains are a collage of magmatic arc, accretionary wedge, ocean basin, and other eugeosynclinal rocks formed during outboard growth of the western North American margin. This study focuses on greenstones in the Sawyers Bar area that are intercalated with limestone, argillite, and chert containing radiolaria of late Permian through early Jurassic age (Blome & Irwin, 1983). The cross-cutting mid-Jurassic English Peak and Russian Peak plutons (U–Pb zircon ages of ≥164 and 159 Ma, respectively; Wright & Fahan, 1988) bracket the end of greenstone eruption; ophiolitic plagiogranite from the region south of Fig. 1 yielded a strongly discordant U–Pb

* Now at Department of Geosciences, University of Arizona, Tucson, AZ 85721, USA.

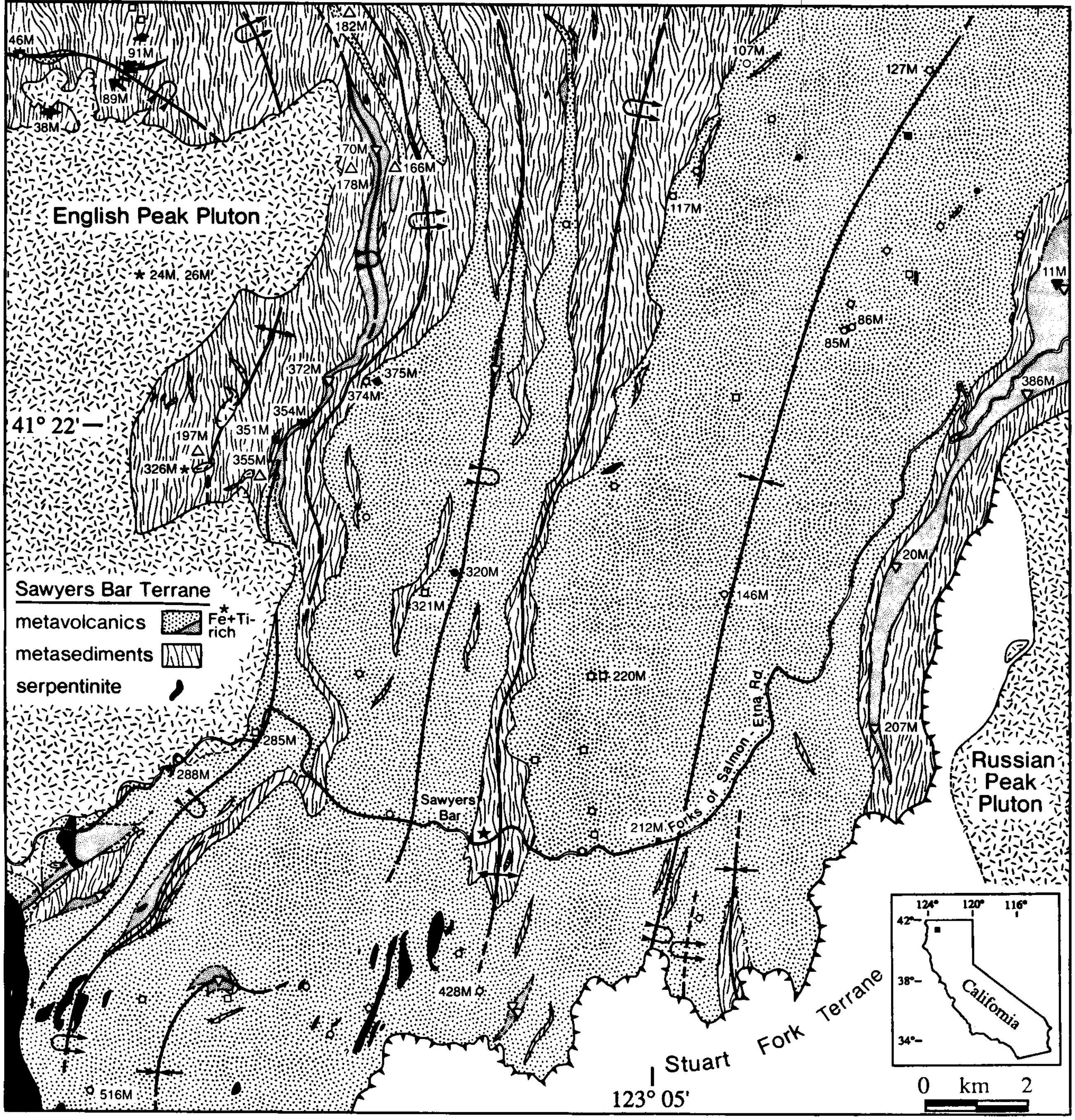

Fig. 1. Geology of the Sawyers Bar area, showing locations of samples. A preliminary version of a portion of this map, including a cross-section, was presented by Ernst (1987). Traces of axial planes are highly interpretive. Sawyers Bar is indicated by a black star. Sample symbols for this illustration (and for Figs 3–11) are as follows: triangles = darker coloured, Ti-rich metavolcanic rocks; circles = lighter coloured, Ti-poor metavolcanic rocks; squares = hypabyssal rocks; filled symbols = Mg-rich ('komatiitic') meta-igneous rocks; unfilled symbols = normal (basaltic) meta-igneous rocks.

zircon age of 310–265 Ma, indicating that eruption may have begun in Permo-Triassic time (Ando *et al.*, 1983). These rocks were thrust eastward beneath the Stuart Fork terrane, a late Triassic subduction complex (Goodge, 1989) prior to the emplacement of the mid-Jurassic plutons.

Much of the study area (Fig. 1) consists of massive to weakly foliated, sparsely pillowed flows and hypabyssal bodies of highly magnesian to tholeiitic basalt composition (Ernst, 1987). They are divided into two groups: darker coloured, high-Ti (>2.0 wt% TiO_2) rocks and lighter coloured, low-Ti (<1.5 wt% TiO_2) rocks. Those of the first group are enriched in light rare-earth elements (LREE), P, Hf, Zr, Ta, Nb, Fe, and Ti, and compositionally resemble alkalic ocean-island basalts, whereas the second group shares trace-element affinities with immature arc tholeiites (Ernst *et al.*, 1991). A significant portion of both the Ti-rich and Ti-poor samples have major-element concentrations appropriate for komatiitic basalts (Arndt & Nisbet, 1982a, b)—up to 18 wt% MgO and CaO/Al_2O_3 ratios ⩾1 (Ernst, 1987). Flows interfinger with quartzo-feldspathic detrital strata and chert interpreted as distal turbidites. The related hypabyssal rocks intrude the flows and sedimentary rocks. Because the metamorphosed dykes and sills are chemically indistinguishable from the Ti-poor extrusive rocks, the entire Ti-poor sequence is permissibly coeval.

The structure of the region is interpreted as several, kilometre-scale or larger, west-vergent synforms and antiforms (Ernst, 1987). Indistinct axial-planar foliation dips steeply to the ENE. Compositional layering in the metasedimentary strata parallels contacts with intercalated metavolcanic rocks. A preliminary geological map is presented as Fig. 1.

The greenstones are texturally complex, having undergone eruption, possible submarine alteration, regional metamorphism, and local contact metamorphism. 'Submarine' alteration is used throughout this paper to indicate any kind of chemical change in the submarine realm, regardless of whether it is associated with ridge-crest hydrothermal activity, the construction of a magmatic arc, or the formation of an ocean island. Evidence for submarine alteration comes primarily from consideration of the bulk-rock compositions and oxygen isotopes. A regionally extensive biotite-zone greenschist facies to prehnite–actinolite facies metamorphism is recognized, by both textures and compositions, in foliated rocks distant from plutons. For example, prismatic igneous amphiboles are overgrown by nematoblastic amphibole zoned toward actinolite. Regional metamorphism was followed by contact metamorphism to amphibolite facies during intrusion of the mid-Jurassic English Peak and Russian Peak calc-alkaline plutons. Contact metamorphosed samples are recognized by hornfelsic textures and distinctive compositional zoning of amphibole and plagioclase. Amphiboles in contact aureoles consist of prismatic pargasite rims on actinolite cores that had developed during the regional metamorphism. Three to four kilometres from the plutons, contact metamorphism is not discernible in the mineral parageneses or compositions, and regional metamorphic minerals are well preserved. Scattered local crystallization of pumpellyite and zeolite minerals was associated with or followed contact metamorphism. A description and discussion of these features forms the bulk of this contribution.

During metamorphism, primary textures were partially to completely recrystallized, and samples containing relict igneous crystals are sporadically distributed throughout the study area (Fig. 2). The best preserved textures in hypabyssal rocks are subophitic to diabasic, with *c.* 100-μm elongate plagioclase laths embedded in larger clinopyroxene crystals. Relict igneous phases compose 0–70 vol% of each sample, indicating that some rocks may have been nearly holocrystalline, others perhaps glassy. Igneous crystals preserved in the metavolcanic rocks include clinopyroxene, hornblende, plagioclase, spinel, apatite, and possibly anorthoclase. Only relict clinopyroxene, hornblende, and plagioclase are abundant. This mineral assemblage is similar to Archaean komatiitic basalts, which contain predominantly clinopyroxene and minor olivine (Cameron & Nisbet, 1982), but the presence of hornblende, apatite, and anorthoclase is quite unlike komatiitic basalts.

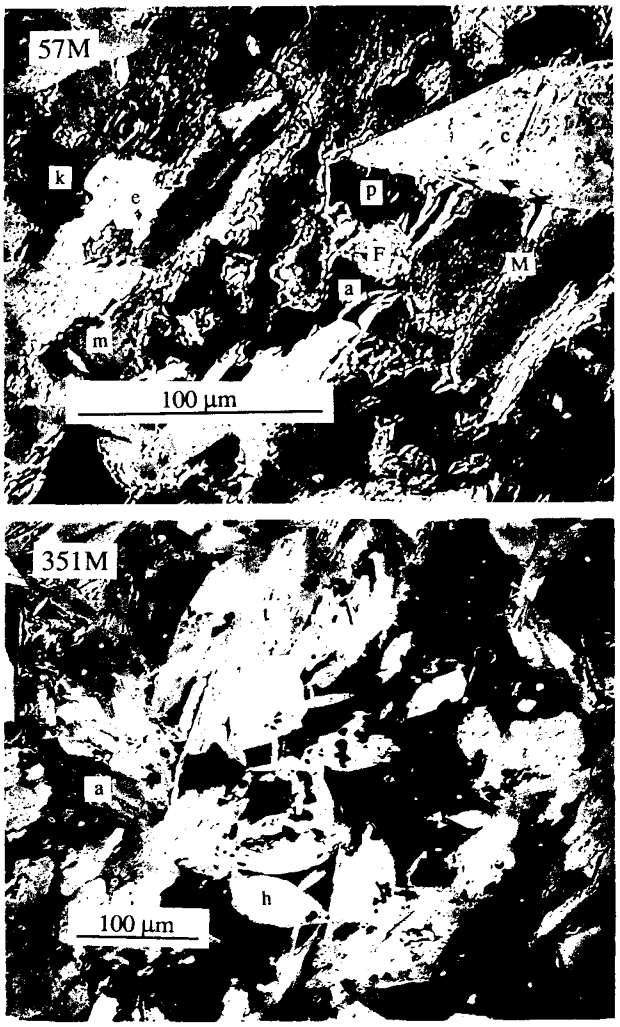

Fig. 2. Back-scattered electron micrographs of regionally metamorphosed metavolcanic rocks. 57M: intergrowth of actinolite (c), Fe-chlorite (F), Mg-chlorite (M), albite (a), andesine (p), epidote (e), muscovite (m), and microcline (k); indications of disequilibrium include patchy zonation in actinolite, two kinds of chlorite, and two kinds of plagioclase. 351M: two kinds of igneous amphibole, tschermakitic hornblende (t) and magnesio-hastingsite (h), overgrown by actinolitic hornblende (a) in a dark matrix of plagioclase, microcline, biotite, muscovite, chlorite, and quartz.

METASOMATISM AND CRYSTAL ACCUMULATION

Several different approaches were used to identify the origin of the 'komatiitic' geochemical signature of the Sawyers Bar greenstones: (i) correlation of oxygen isotopic values with metamorphic mineral modes and bulk-rock composition; (ii) identification of elemental variations that are atypical of igneous rocks; and (iii) determination of original bulk-rock compositions based on compositions and modes of relict igneous minerals. If such changes can be identified, then it should be possible to 'see through' any metasomatic veil back to the igneous bulk compositions and clarify the igneous petrogenesis of these unusually MgO-rich rocks. We interpret the variable chemical and isotopic compositions of the metavolcanic rocks to reflect a combination of three distinct processes: (i) limited igneous compositional variation mainly involving cumulus hornblende and/or augite; (ii) minor metasomatism accompanying submarine alteration and regional metamorphism; and (iii) oxygen isotopic exchange and very limited chemical exchange with metasedimentary rocks during contact metamorphism.

Bulk-rock compositions were presented and discussed in detail by Ernst (1987) and Ernst *et al.* (1991); only those aspects relevant to evaluating metasomatism and crystal accumulation are presented here. Most trace elements within the metavolcanic rocks show systematic relationships with each other (Fig. 3). The trace element concentrations are probably related to igneous processes, but the igneous major elemental ratios may not have been preserved during metamorphism. The Ti-rich rocks have trace element concentrations typical of alkalic within-plate lavas, including elevated Ta and Nb contents, and the Ti-poor rocks are similar to immature arc lavas, including having reduced Ta and Nb values (Ernst *et al.*, 1991). Trace element concentrations are unlike komatiites or komatiitic basalts, which, for example, contain <16 ppm Ce (Beswick, 1982) and <140 ppm Zr (Arndt & Nesbitt, 1982). Moreover, the trace element concentrations are incompatible with back-arc basin basalts, boninites, or mid-ocean ridge basalts (Ernst *et al.*, 1991). The

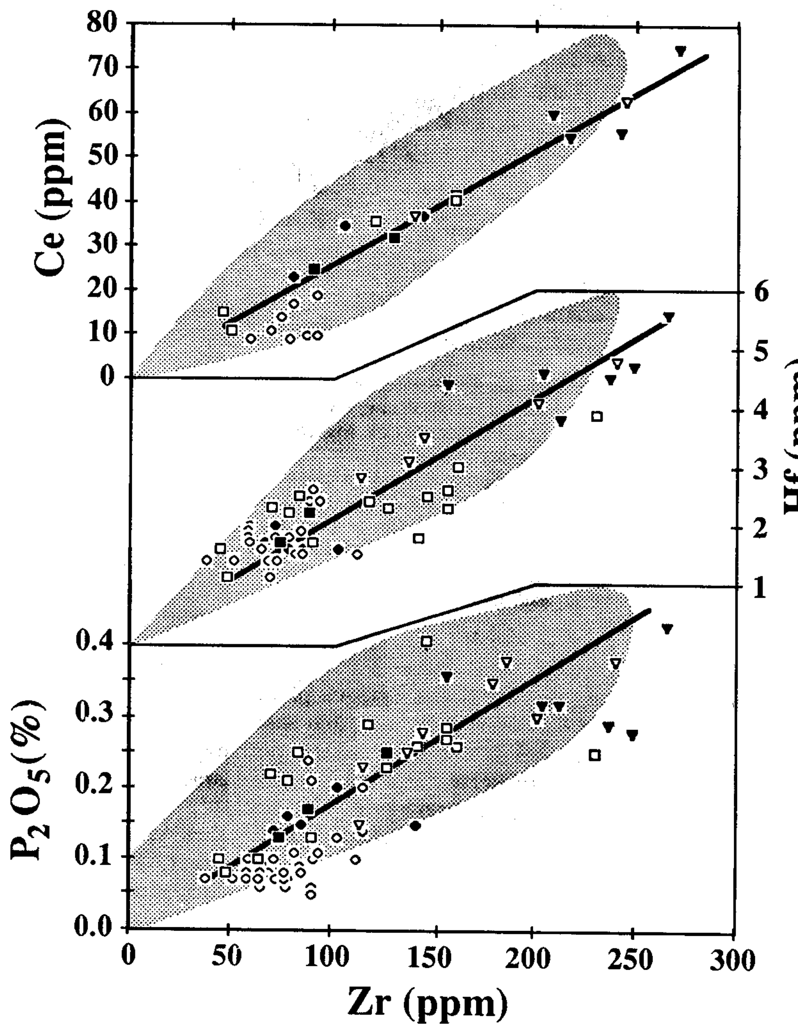

Fig. 3. Systematic bulk-rock variations of P, Hf, and Ce concentrations with respect to Zr. Typical concentrations of P, Hf, Ce, and Zr in basaltic rocks are shaded (B. R. Hacker literature survey, unpublished). Symbols as in Fig. 1.

concentrations of all minor elements that were measured are comparable to alkalic within-plate lavas (Ti-rich rocks) and immature arc lavas (Ti-poor rocks), as detailed by Ernst *et al.* (1991).

Whereas minor and trace element concentrations show systematic variation with respect to fractionation indices such as Zr (Fig. 3) (Ernst *et al.*, 1991), most of the major element concentrations, although within the range of unaltered worldwide volcanic rocks, show considerably more scatter (Fig. 4) (Ernst *et al.*, 1991). Some of the scatter could be due to fractionation or assimilation; however, these greenstones are fairly primitive, and variation is more likely the result of metasomatism or crystal accumulation. The primitive nature is indicated by Cr contents of 400–1000 ppm, Ni contents of 130–500, and Mg/(Mg + Fe) ratios of 0.55–0.65, for the most magnesian lavas (Ernst *et al.*, 1991). Without unaltered rocks from the same eruptive suite to serve as a basis for comparison, means for assessing major element metasomatism are limited. Compared to worldwide volcanic rocks, some of the Sawyers Bar volcanic rocks have unusually low amounts of Al_2O_3 or Na_2O, elevated MgO, and variable K_2O concentrations (Fig. 4). Zr contents are clearly correlated with other 'immobile' trace elements (Fig. 3) and are probably igneous, hence the unusual Al_2O_3, MgO, Na_2O and K_2O contents may reflect metasomatism or the presence of cumulus phases. Figure 4 shows that some samples may be depleted by as much as 3 wt% Al_2O_3, 1.5 wt% Na_2O and 0.5 wt% K_2O, and elevated by as much as 6 wt% MgO and 0.5 wt% K_2O. No other major elements are present in concentrations atypical of worldwide volcanic rocks. Although the depleted Al_2O_3 and elevated MgO contents may have contributed to the 'komatiitic' character of these basalts, many of the samples (including some with high MgO contents) are not demonstrably different from worldwide volcanic rocks. Thus, the 'komatiitic' character of these rocks, including the elevated MgO, Ni, and Cr contents, may be the result of some igneous process.

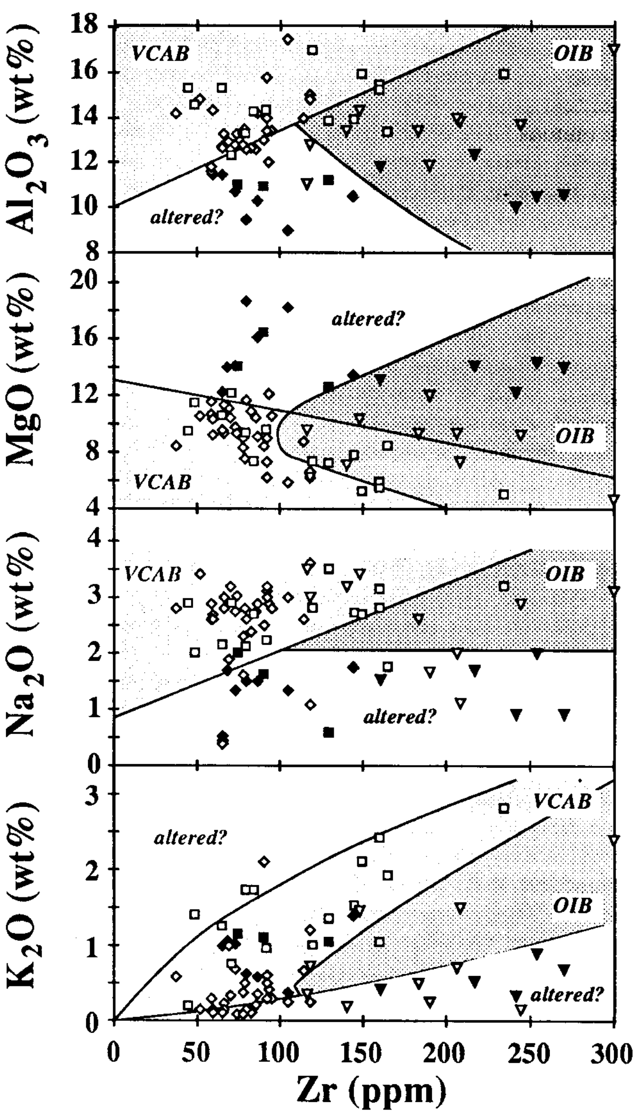

Fig. 4. Comparison of Sawyers Bar greenstone major-element concentrations with worldwide volcanic rocks. Shaded fields labelled 'VCAB' and 'OIB' show typical values of intraoceanic and continental arc rocks and ocean-island basalts, respectively (B. R. Hacker literature survey, unpublished). Symbols as in Fig. 1.

Bulk-rock Cr contents decrease with increasing Zr and decreasing MgO, suggesting that clinopyroxene or hornblende fractionation or accumulation influenced the compositional evolution (Ernst *et al.*, 1991). Similar behaviour of Ni also suggests that olivine, clinopyroxene, or hornblende fractionation or accumulation was important. Element-ratio diagrams rule out the participation of olivine and plagioclase, but support the contention that clinopyroxene or hornblende were fractionating or accumulating phases (Ernst *et al.*, 1991).

To evalute whether the elevated MgO contents could also have been affected by clinopyroxene or hornblende fractionation or accumulation, it is necessary to determine whether the excess MgO contents of Sawyers Bar greenstones are correlated with the volume per cents of igneous hornblende or pyroxene. In worldwide volcanic arc rocks, MgO is correlated with Cr_2O_3 (Fig. 5a). At a given Cr_2O_3 content, the Sawyers Bar rocks are displaced to higher MgO contents—toward the compositions of 'relict hornblende and pyroxene'—by comparison with worldwide volcanic rocks. Using the relationship between MgO and Cr_2O_3 shown by the diagonal line in Fig. 5(a), 'excess' MgO for a given Cr_2O_3 content was estimated for each sample (Fig. 5b). Figure 5(b) shows that the magnitude of 'excess' MgO is correlated with the abundance of igneous hornblende. Moreover, the magnitude of the excess is qualitatively similar to that suggested in Fig. 4. To avoid some of the potential circularity in Fig. 5(a, b) (circular because hornblende contains substantial Cr_2O_3 as well as MgO), the 'excess' MgO derivation has been repeated using Hf in place of Cr_2O_3 in Fig. 5(c); the results are in agreement. Similar diagrams based on correlation of 'excess' MgO with the volume per cent of pyroxene yield similar results,

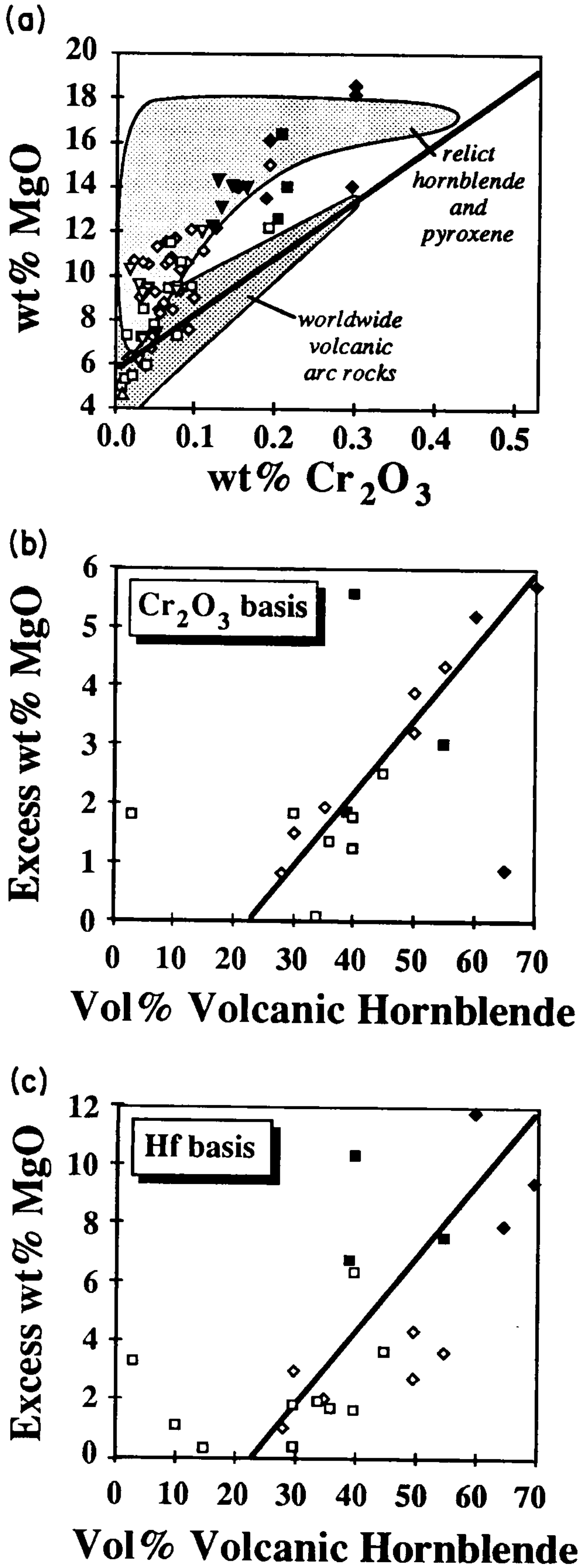

Fig. 5. (a) Relationship of MgO to Cr_2O_3 content in volcanic rocks. Compositions of worldwide arc volcanic rocks (B. R. Hacker literature survey, unpublished), and Sawyers Bar relict igneous hornblende and pyroxene crystals are shaded. Diagonal line shows approximate relationship between MgO and Cr_2O_3. (b) 'Excess' MgO for a given Cr_2O_3 content in hornblende-bearing samples is correlated with the volume per cent of igneous hornblende. The scale of the vertical axis is related to the slope of the diagonal line in Fig. 5(a). (c) 'Excess' MgO for a given Hf content in hornblende-bearing samples is correlated with the volume per cent of igneous hornblende. Symbols as in Fig. 1.

suggesting that bulk-rock compositions are not quenched liquid compositions, but contain a contribution from cumulus amphibole and/or pyroxene. Moreover, there is no need to invoke metasomatism to account for the high MgO contents of these rocks, although metasomatism may be responsible for the unusual Al_2O_3, Na_2O, and K_2O contents.

Oxygen isotopes

Oxygen isotope bulk-rock compositions were measured in 21 samples to assess the degree of metasomatism in the metavolcanic rocks. Analyses were done by fluorination with ClF_3 (Bothwick & Harmon, 1982) and conventional mass spectrometry; reproducibility was ±0.2%.

Oxygen isotope systematics are disturbed from plausible igneous compositions in all analysed metavolcanic rocks (Table 1). Measured $\delta^{18}O_{SMOW}$ values increase toward granitoid plutons (Fig. 6). Samples more than 3 km from the plutons have $\delta^{18}O$ values of +8.7 to +11.4‰, whereas samples closer to these late intrusions are as heavy as +15.9‰. The English Peak pluton yields bulk rock $\delta^{18}O$ values of +11.3‰ (nearly unaltered sample) to +10.4‰ (sample adjacent to and contaminated by wall rocks); samples of metasedimentary rocks intercalated with the metavolcanic rocks have $\delta^{18}O$ values ranging from +12.4 to +17.9‰. Hence, it may be concluded that the heavy oxygen values noted in the greenstones adjacent to the plutons were a consequence of exchange with fluids derived from the interlayered ^{18}O-rich metasedimentary rocks. In spite of the observation that $\delta^{18}O$ values are dependent on the proximity of samples to plutons, we are unable to demonstrate that other elements behave in a similar fashion. This suggests that any shifts in bulk compositions away from probable igneous values are unrelated to contact metamorphsim.

Although there are many uncertainties, low-T (<250° C) submarine hydrothermal alteration typically enriches ^{18}O in shallow (<2–3 km) mafic rocks from protolith values of +5 to +7‰ (Taylor, 1968; Beaty & Taylor, 1982) to final values of +7 to +12‰ (e.g. Bowers & Taylor, 1985; Muehlenbachs, 1986). Deeper level (hotter) hydrothermal exchange should produce ^{18}O depletions at moderate to high fluid-to-rock values. The +8 to +11‰ range in the metavolcanic rocks away from the granitic plutons is compatible with equilibration with seawater (0‰) in the 100 to 200° C range. An alternative origin with higher temperature exchange would require a considerably large

Table 1. $\delta^{18}O$ bulk-rock values for metamorphosed igneous rocks, associated sedimentary rocks, and the English Peak pluton.

Rock type	Sample	$\delta^{18}O$ (‰)	
TiO_2-rich volcanic	91M†	15.89	
	170M	13.04	
	201M	10.84	
	207M	12.10*	
	354M†	12.85	
	372M	11.32	
	386M	10.80	
TiO_2-poor volcanic	46M	13.81	
	86M	8.69	
	92M†	14.22	
	117M	11.15	
	146M	9.36	
	288M	14.89*	
	374M	13.02	
	516M	10.58*	
Hypabyssal	220M	11.37	
	285M	11.46*	
Sedimentary	134M	16.63	
	166M	14.67	
	178M	14.87	
	182M	12.36	
	197M	17.94	
	355M	13.28	
English Peak pluton	24M	11.27	(quartz = 13.53)
	26M	9.0*	(quartz = 13.98)
	326M	10.4*	

* Average of two analyses.
† 'Komatiitic' sample.

volume of water isotopically heavier than seawater. No adequate source for such a fluid is apparent. This suggests that oxygen isotopic exchange during regional metamorphism was minor. Integrated fluid-to-rock ratios during submarine hydrothermal exchange must have been $>c.$ 5 in order to achieve the observed isotopic shifts. The

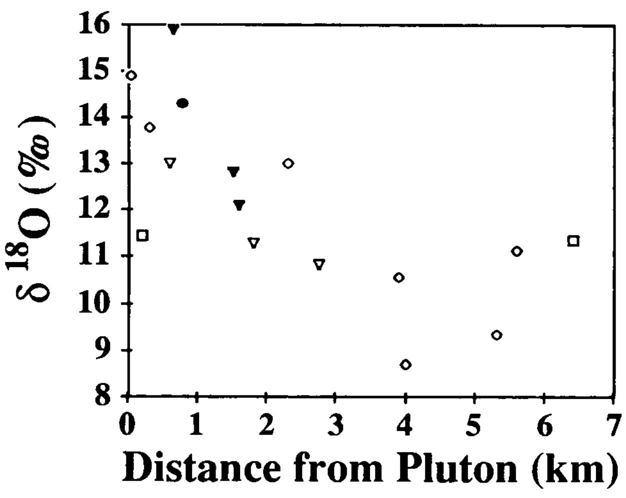

Fig. 6. Relationship between bulk-rock oxygen isotope compositions of metavolcanic rocks and proximity to calc-alkaline English Peak and Russian Peak plutons. Symbols as in Fig. 1.

irregular, but substantial MgO enrichment in the metavolcanic rocks and the considerable variability in K_2O and Na_2O, attributed earlier to crystal accumulation, could also have been influenced by the submarine hydrothermal fluids that caused the regional ^{18}O enrichment (e.g. Alt *et al.*, 1986; Seyfried *et al.*, 1988).

The heterogeneous but marked enrichment in $\delta^{18}O$ near the Russian Peak and English Peak plutons is most consistent with a contact metamorphic origin. The large ^{18}O enrichment contrasts with the typical large ^{18}O depletions observed in the aureoles of most epizonal intrusions (Criss & Taylor, 1986). Calculated waters would have had $\delta^{18}O = +9$ to $+12$‰ at the conditions of metamorphism, much heavier than any plausible surface-derived water. The only reasonable source of heavy oxygen is the intercalated metasedimentary sequence (see Table 1). Metasedimentary rocks are more abundant in the areas near the intrusive contacts, the general areas of ^{18}O enrichment in the greenstones. Local evidence for metasediment–metaigneous exchange (described above) and the lack of other adequate sources of heavy oxygen require re-equilibration on the scale of 10^1–10^3 m. This exchange was probably facilitated by local fluid circulation driven by emplacement of the English Peak and Russian Peak plutons; however, the volume of introduced fluid must have been small relative to the volume of the altered rocks because of the areally limited ^{18}O enrichment.

Given the subequal amounts of exposed metasedimentary and metavolcanic rocks, this postulated exchange should have decreased the $\delta^{18}O$ of the metasedimentary rocks. Such a decrease is difficult to document given the substantial variation in sedimentary oxygen isotope compositions; however, it is possible that much of the metasedimentary section could have had original compositions in excess of +20‰ as is typical of cherty, calcareous, and clay-rich sediments (Hoefs, 1987) and has now been shifted to *c.* +15‰ (Table 1) (Ernst *et al.*, 1991).

METAMORPHIC MINERALS

Thirty-seven low-variance, mineralogically representative samples were selected for back-scattered electron microscopy and electron-probe microanalysis to evaluate metamorphism of these unusually magnesian metavolcanic rocks.* Sample localities are indicated on the geological map of Fig. 1. Mineral analyses were made with a four-spectrometer Cameca Camebax electron-probe microanalyser using well-characterized natural and synthetic mineral standards whose major element concentrations are reproducible to better than ±2% for major elements and ±10% for minor elements. Textural analysis and spot selection were performed in back-scattered-electron mode. The electron beam diameter was 2 μm at 15-kV accelerating voltage and 10–15-nA sample current on minerals. Counting periods of 20 s for peak intensities

* Detailed chemical analyses of minerals from the Sawyer's Bar Area are available, on request, from the first author.

and 10 s for background intensities were made for each of 10 elements. Detection limits at these conditions are a function of mineral composition, but conservative limits are 0.02 wt% for SiO_2, Al_2O_3, TiO_2, Cr_2O_3, and MnO, 0.03 wt% for FeO, MgO, and CaO, 0.04 wt% for K_2O, and 0.05 wt% for Na_2O. Analyses of inhomogeneous grains are presented individually. All mineral formulae were calculated by the method of Laird & Albee (1981a, b), except as noted. Amphibole names follow the convention of Rock & Leake (1984).

Regional metamorphic assemblages span upper greenschist to prehnite–actinolite facies. The low-variance regional greenschist facies assemblage is actinolitic hornblende + phengite + epidote + chlorite + albite + microcline + quartz + titanite + hematite in low-Ti rocks; biotite is also present in low-variance assemblages developed in high-Ti rocks. The low-variance, regionally developed prehnite–actinolite facies assemblage is actinolite + phengite + epidote + chlorite + albite + prehnite + titanite + quartz. Contact metamorphic assemblages nearest to plutons contain pargasitic hornblende ± clinopyroxene + calcic plagioclase + epidote + muscovite + biotite + titanite.

Detailed microprobe traverses from amphibole cores to rims reveal that three stages of amphibole growth are represented in the greenstones. Some amphiboles contain an igneous pargasitic hornblende core overgrown by a regional metamorphic rim zoned outward to actinolite, in turn overgrown by a contact metamorphic rim zoned outward to pargasite. Amphiboles that grew during regional metamorphism consist of discrete fibrous neoblasts in the groundmass and rims on stout prisms of volcanic hornblende and pyroxene. Most are subhedral to euhedral, lath-shaped to equant crystals 100–300 μm in length, and are principally actinolite. Most amphiboles grown during regional metamorphism display decreases in Na^{M4}, $Na^A + K$, $Al^{VI} + Fe^{3+} + Ti$, and Al^{IV}, from core to rim (Fig. 7a). This zonation may have resulted from some combination of two processes: continuous equilibration of the amphibole rims during decreasing temperature, or disequilibrium growth.

Contact metamorphic amphiboles form overgrowths on regional metamorphic amphiboles and are zoned smoothly from actinolitic cores to paragasitic hornblende rims (Fig. 7b). One contact metamorphosed sample (46M) close to English Peak pluton contains the texturally equilibrated pair magnesio-cummingtonite + magnesio-hornblende associated with andesine and Mg-rich chlorite. Most calcic amphiboles produced during contact metamorphism display continuous increases in $Na^A + K$, $Al^{VI} + Fe^{3+} + Ti$, Al^{IV}, Na/Ca, and Al/Si, from core to rim (Figs 7 & 8)—exactly opposite to the regional metamorphic trend. Approaching the granitoids, SiO_2 and CaO contents of regional actinolitic amphibole rims begin to decline sharply beginning about 3–4 km from plutons as these phases are overprinted; Al_2O_3. TiO_2, Na_2O, and K_2O contents concomitantly increase (Figs 9 & 10a, b). The mechanism for the incorporation of the Al_2O_3 is principally through the tschermak and edenite substitutions (Fig. 7b), compatible with higher temperatures near the plutons. The MgO contents of amphiboles in the greenstones are related to bulk-rock magnesia contents. No other elements in amphiboles are correlated with bulk-rock composition.

Biotite is present in fewer than half the metabasaltic samples studied, primarily in Ti-rich metamorphosed extrusive rocks. The biotite occurs as subhedral plates 20–80 μm in length. Biotite ranges in composition from $K_{1.0}Mg_{1.3}Fe_{1.3}Cr_{0.0}Ti_{0.2}Al_{0.2}(Al_{1.2}Si_{2.8})O_{10}(OH)_2$ to $K_{1.0}Mg_{1.7}Fe_{0.8}Cr_{0.1}Ti_{0.0}Al_{0.4}(Al_{1.1}Si_{2.9})O_{10}(OH)_2$. MnO, CaO, and Na_2O are minor constituents, whereas Cr_2O_3 accounts for as much as 1.1 wt% in biotite. There are too few biotite analyses to evaluate whether there is any systematic regional variation in the composition.

Phengite occurs in most greenstone samples as 10–50-μm-sized subhedral platelets produced by recrystallization of feldspar. White mica ranges in composition from $K_{0.8}Mg_{0.3}Fe_{0.1}Al_{1.5}(Al_{0.6}Si_{3.4})O_{10}(OH)_2$ to $K_{0.9}Mg_{0.1}Fe_{0.0}$-$Al_{1.8}(Al_{0.9}Si_{3.1})O_{10}(OH)_2$. TiO_2, Cr_2O_3, MnO, CaO, and Na_2O are all minor constituents of the phengite platelets. The MgO contents of white micas (0.6–4.3 wt%) are weakly correlated with bulk-rock MgO contents. Phengites near granitic plutons in the contact aureoles contain more TiO_2 and less SiO_2 than those generated during the earlier regional metamorphism (Fig. 11).

Chlorite is present in every sample studied, typically as subhedral flakes 20–80 μm in length. Chlorite TiO_2, Cr_3O_3 and MgO contents depend on bulk-rock composition. No systematic regional variation in chlorite composition was detected, and the range in composition of chlorite platelets from a single sample is comparable to the variation in compositions of all analysed crystals. Much of the chemical variation can be accounted for by substitution of $(Mg,Fe^{2+},Mn)Si$ for $(Cr,Al^{VI})Al^{IV}$, producing Al^{VI} variation of 1.2–1.5 atoms per formula unit (p.f.u.). MnO and Cr_2O_3 are present in minor quantities.

Plagioclase crystals interpreted as volcanic, regional metamorphic, and contact metamorphic are all present. Igneous plagioclase crystals, An_{29-50} (Ernst *et al.*, 1991), are typically long and slender, oscillatorily zoned, and intimately intergrown with pyroxene or amphibole. Metamorphic plagioclase occurs in nearly all samples within healed cracks in relict igneous laths and as neoblasts within or adjacent to precursor igneous crystals. Most plagioclase crystals are 20–60 μm in diameter, anhedral, and equant. The compositions of plagioclase grains do not depend on bulk-rock compositions, except in contact metamorphosed rocks lacking quartz where plagioclase CaO correlates with bulk rock CaO. Individual albite (An_{01-09}), individual oligoclase (An_{10-20}), and albite + oligoclase pairs are found in regional metamorphic assemblages (Fig. 10c). Albite + oligoclase pairs in two samples have compositions appropriate for the peristerite gap (Maruyama *et al.*, 1982): $An_{03\pm00} + An_{18\pm01}$ and $An_{04\pm00} + An_{18\pm01}$ (Fig. 10c). In contact metamorphosed rocks within 2 km of calc-alkaline plutons, plagioclase ranges from An_{20} to An_{98} (Fig. 10c). Contact metamorphic plagioclase crystals contain minor but measurable amounts of TiO_2, Cr_2O_3, and MnO; Fe_2O_3, MgO, and K_2O are more abundant.

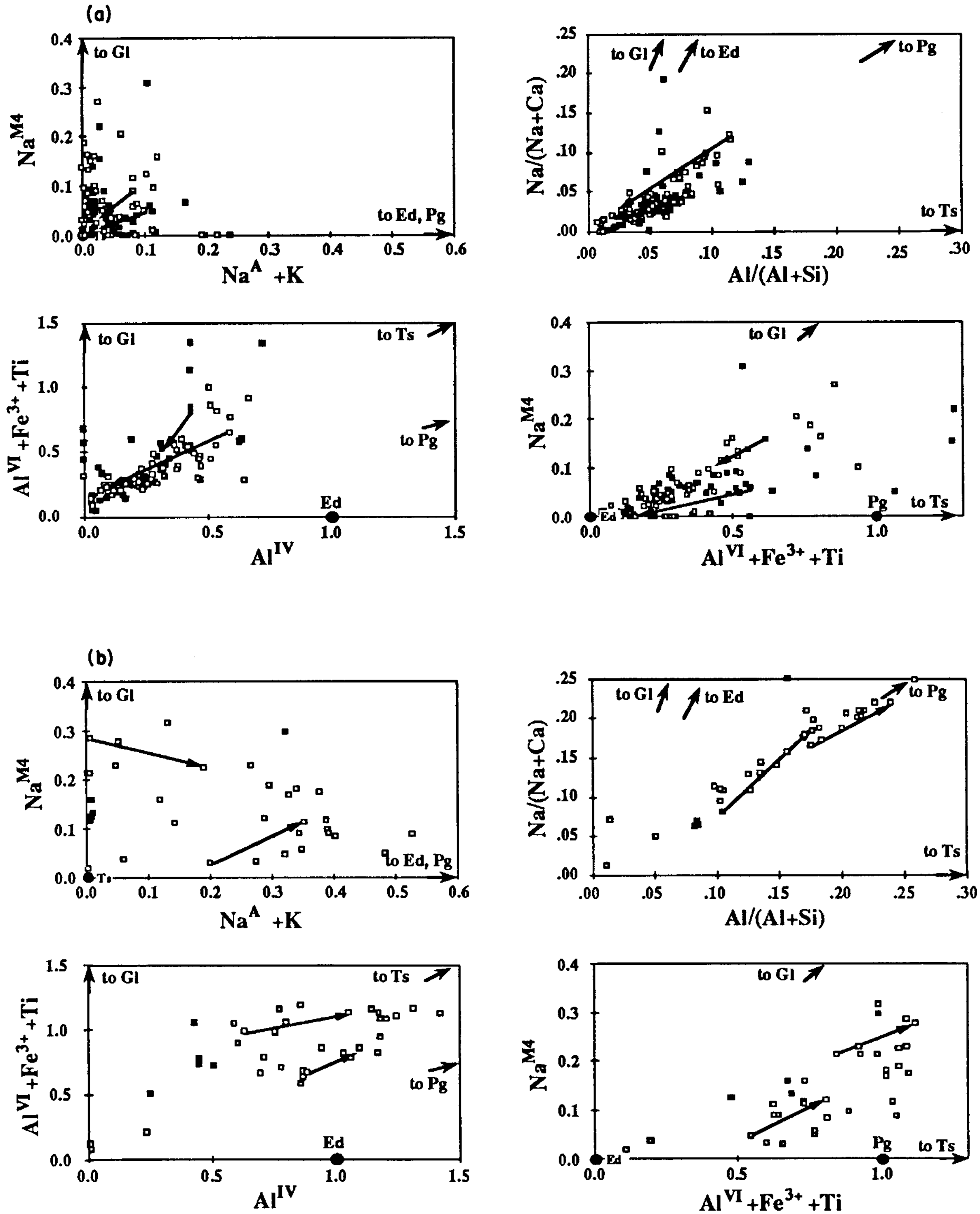

Fig. 7. Compositions of amphiboles (atoms per 23 oxygens) developed during (a) regional and (b) contact metamorphism plotted on discriminant diagrams of Laird & Albee (1981b). Tschermakite substitution produces a 1 : 1 slope on the $Al^{VI} + Fe^{3+} + Ti$ versus Al^{IV} diagram, and glaucophane substitution produces a 1 : 1 slope on the Na^{M4} versus $Al^{VI} + Fe^{3+} + Ti$ diagram. Typical core-to-rim zonations are shown by arrows. Filled symbols indicate amphiboles that coexist with a Ca–Al silicate, chlorite, albite, quartz, and a Ti-phase; unfilled symbols indicate amphiboles from higher variance assemblages. End-member amphibole compositions shown are Ed = edenite, Gl = glaucophane, Pg = pargasite, and Ts = tschermakite.

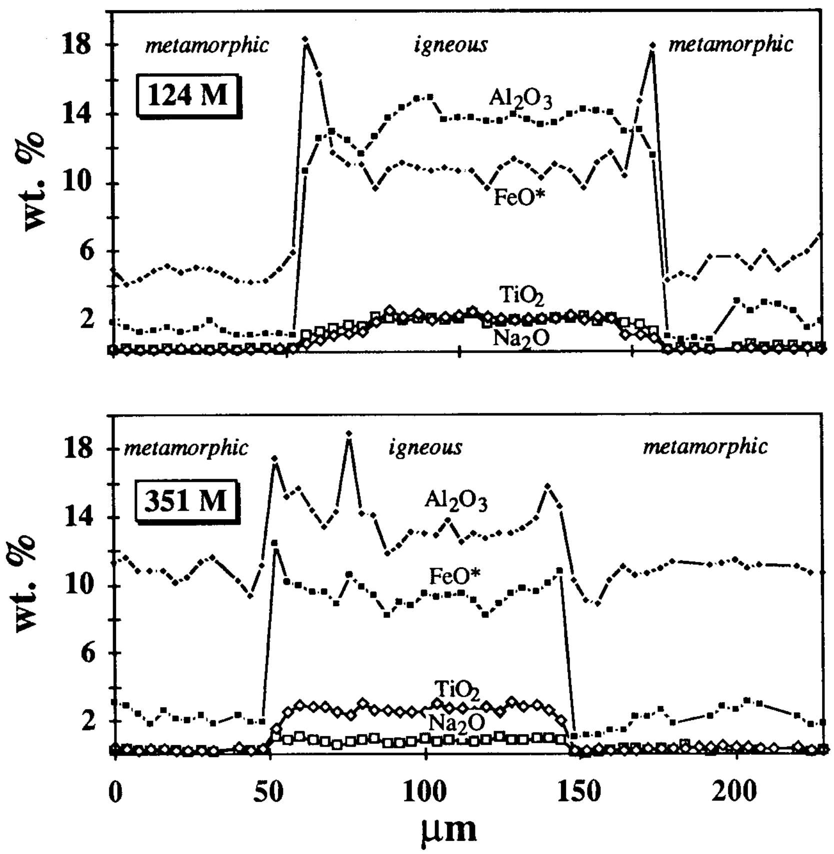

Fig. 8. Compositional profiles of single amphibole crystals from two samples. The amphibole cores formed by crystallization from a magma and the rims formed during regional metamorphism.

Metamorphic microcline ($An_{00}Or_{97-98}Ab_{02-03}$) is present in more than half the samples studied, and is found in all samples with ≥1.5 wt% K_2O. It typically occurs adjacent to phengite crystals in 10–15-μm-diameter, anhedral, equant crystals, and consequently was identified only by back-scattered electron microscopy. Fe_2O_3 (≤0.5 wt%) and MgO (≤0.3 wt%) are abundant minor elements, whereas TiO_2, Cr_2O_3, and MnO are less important.

Epidotes are widespread euhedral prismatic to subhedral equant minerals 50–100 μm in diameter. Their compositions are not related to bulk-rock compositions, and show no systematic spatial variation. Epidotes with cores that contain 12–31 mol% pistacite, $Ca_2Fe_3Si_3O_{12}(OH)$, are zoned to slightly more aluminous rims (11–30 mol% pistacite), and cores with 3–13 mol% pistacite are overgrown by more ferruginous rims (12–19 mol% pistacite). TiO_2, Cr_2O_3, MnO, MgO, Na_2O and K_2O are present in minor or insignificant amounts.

Pumpellyite was found in three samples, filling cracks in hornblende in one contact metamorphosed rock, and in veins in two regionally metamorphosed rocks—hence it clearly grew later than or during waning stages of those metamorphic events. The composition varies from $Ca_{3.7}Mg_{0.5}Fe_{0.5}Al_{5.1}Si_{6.1}O_{22}(OH)_5$ to $Ca_{3.8}Mg_{0.8}Fe_{0.2}Al_{5.0}$-$Si_{6.0}O_{22}(OH)_5$. In this study, pumpellyite analyses were normalized to 24.5 oxygen atoms pfu (after Yoshiasa & Matsumoto, 1985). Prehnite, $Ca_{1.9}(Fe, Al)_{2.0}Si_{3.0}O_{10}(OH)_2$ with $X_{Fe} = Fe/(Al + Fe) = 0.00–0.07$, was found in 20 samples, including hornfelsic greenstones bordering the English Peak pluton; in one sample it forms pseudomorphs after epidote. Zeolite minerals occur in two samples. The principal constituents are SiO_2, Al_2O_3, CaO, and Na_2O, and the different crystals within single samples are quite variable in composition.

Titanite and ilmenite are widespread titaniferous phases forming 20–50-μm anhedral, equant crystals; titanite is typically an alteration product of ilmenite. Hematite, chalcopyrite, and pyrite are scattered trace phases in most samples.

CONDITIONS OF METAMORPHISM AND REGIONAL SIGNIFICANCE

Textures and mineral compositions suggest the following sequence of events: (i) the metavolcanic rocks were extruded and altered in a submarine environment coincident with deposition of the intercalated deep-water sedimentary rocks (Ernst *et al.*, 1991); (ii) high-grade greenschist (north) to prehnite–actinolite (south) facies regional metamorphism overprinted the entire section during deformation; (iii) the English Peak and Russian Peak calc-alkaline plutons intruded the area, causing hornfelsic contact metamorphism and shifts in oxygen isotopic composition; and (iv) pumpellyite and zeolite

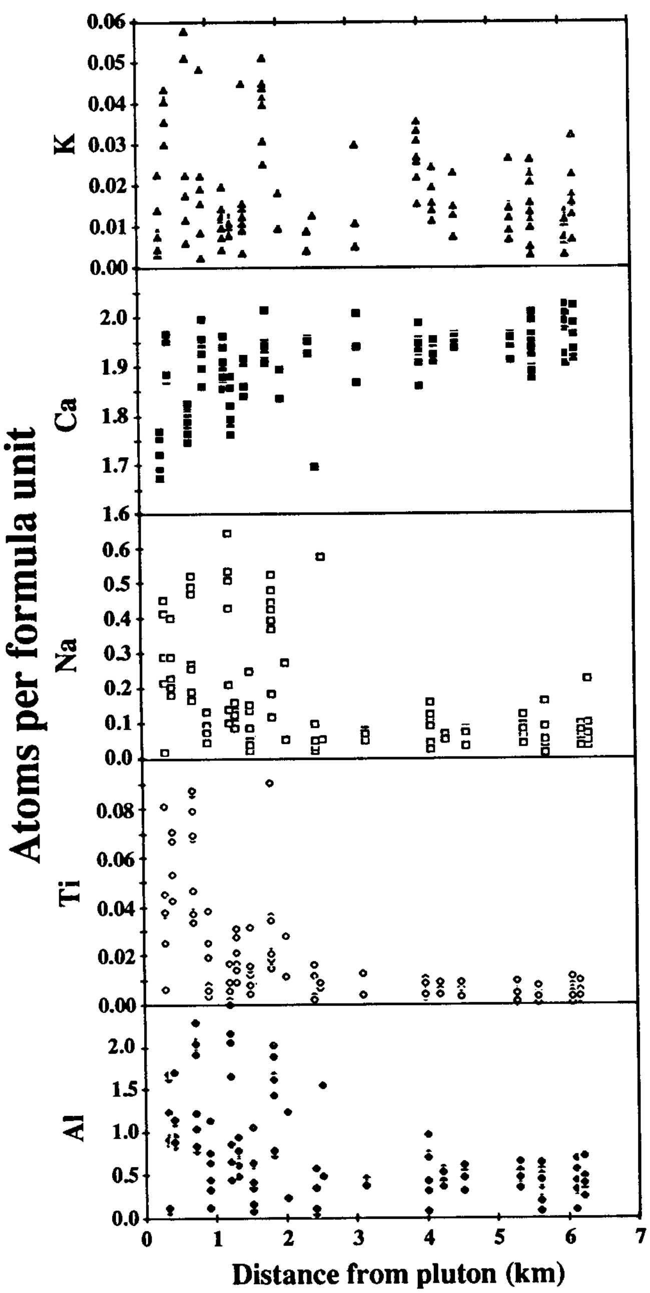

Fig. 9. Changes in compositions of amphiboles (atoms per 23 oxygens) produced by mid-Jurassic English Peak and Russian Peak calc-alkaline plutons; each symbol represents a single analysis and columns of symbols at a given distance from plutons are from a single sample.

growth occurred locally during late-stage retrograde recrystallization. Based on radiometric and fossil ages mentioned in the introduction, the regional metamorphism took place after or during early Jurassic time, and the contact metamorphism is mid-Jurassic in age.

Estimates of physical conditions during metamorphism(s) are possible, based on the observed phase compositions and assemblages (Fig. 12). The presence of epidote + actinolite and the absence of glaucophane suggest that the regionally developed greenschist facies assemblages formed at temperatures between 350 and 550° C. Note, however, that reactions (1) and (2) in Fig. 12 are unreversed and experiments delimiting reaction (2) were unbuffered with respect to f_{O_2} as well. Moreover, experiments on reaction (1) were conducted in the CaO–MgO–Al_2O_3–SiO_2–H_2O (CMASH) system, whereas those on reaction (6) were conducted in the CaO–FeO–Fe_2O_3–Al_2O_3–SiO_2–H_2O (CFASH) system. Epidote + pargasite in contact metamorphic assemblages suggests peak metamorphic conditions between reactions (4) and (6) in Fig. 12.

Laird & Albee (1981b) showed that compositions of metamorphic amphiboles from mafic rocks containing chlorite + epidote + plagioclase + quartz + a Ti-phase are systematic functions of pressure and temperature. The regional and contact metamorphic amphiboles in the Sawyers Bar area all fall within the medium-*P* (kyanite–sillimanite) to low-*P* (andalusite–sillimanite) facies series trends as delineated by Laird & Albee (1981b), Hynes (1982), and Laird *et al.* (1984). The presence of oligoclase + actinolite in the greenstones (Fig. 11) is also compatible with moderate to low metamorphic pressures (Miyashiro, 1973, p. 288; Maruyama *et al.*, 1982).

Liou *et al.* (1985) proposed the existence of the prehnite–actinolite facies to describe assemblages containing prehnite + actinolite + epidote + chlorite + albite + quartz + titanite. This facies is transitional between zeolite or prehnite–pumpellyite to greenschist facies at low pressures, and may correspond to metamorphic temperatures of 200–400° C and pressures of ≤3 kbar (Liou *et al.*, 1987). Rocks containing this assemblage are present in the south-west of the Sawyers Bar area (Fig. 10c).

The Al content in igneous hornblende coexisting with potassium feldspar, quartz, plagioclase, biotite, titanite, ilmenite or magnetite, and silicate liquid can be used to estimate the depth of emplacement of the English Peak pluton. Hornblende cores contain 1.3–1.4 Al atoms p.f.u., and rims have 1.1–1.6 Al atoms p.f.u. Although the total distribution of rim compositions is large, the mean and standard deviation are 1.4 ± 0.14 Al atoms p.f.u. Empirical (Hollister *et al.*, 1987) and experimental calibrations (Johnson & Rutherford, 1989) indicate pressures of 2.6–3.7 ± 1 kbar and 2–2.9 ± 0.5 kbar, respectively, for crystallization of hornblende with 1.4 ± 0.14 Al atoms p.f.u. The experiments were conducted at several oxygen fugacities at pressures as low as 2 kbar and are reversed; the preferred pressure of crystallization is 2–2.9 ± 0.5 kbar (bar 7 in Fig. 12).

In summary, regional greenschist facies metamorphism occurred at temperatures of 350–550° C and moderate to low pressures (*c.* 3 kbar); in contrast, slightly later contact metamorphism occurred at temperatures as high as *c.* 600° C, coincident with crystallization of the English Peak granodiorite at 2–2.9 ± 0.5 kbar. Prehnite–actinolite facies assemblages developed at lower temperatures (200–

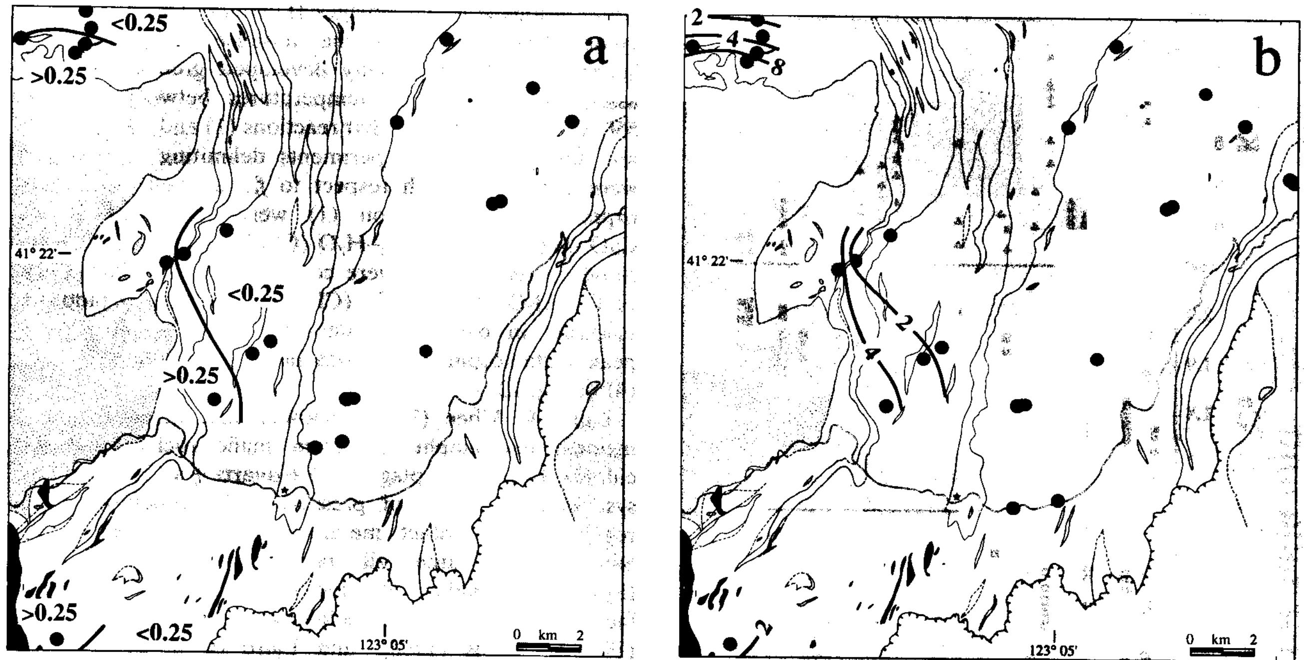

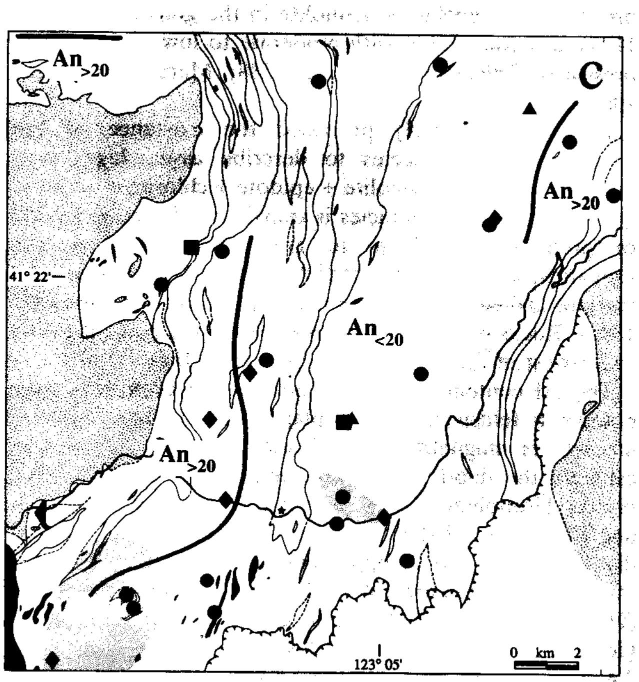

Fig. 10. (a) Contours of wt% TiO_2 in amphibole cores. (b) Contours of wt% Al_2O_3 in amphibole cores. (c) Distribution of metamorphic plagioclase and prehnite. Regional metamorphism: circles indicate albite, squares oligoclase, diamonds albite of any composition + oligoclase of any composition and triangles albite + oligoclase peristerite pairs; shaded area indicates regionally metamorphosed samples containing the lower grade equilibrium pair prehnite + actinolite. Contact metamorphism: solid lines delineate areas near plutons containing plagioclase more anorthitic than An_{20}. Other symbols and contacts after Fig. 1.

400° C) and pressures (≤3 kbar) (Liou *et al.*, 1987). Because these estimates are based on experiments conducted under non-ideal conditions (e.g. some reactions are unreversed, unbuffered, or conducted on simplified synthetic systems), they should be viewed as only approximate.

A mid-Jurassic metamorphism termed the Siskiyou event (Coleman *et al.*, 1988) occurred during and after widespread plutonism in the central Klamath Mountains (Wright & Fahan, 1988; Donato, 1989). Several features suggest that regional metamorphism in the Sawyers Bar area is correlative with the Siskiyou event: (i) early to mid-Jurassic age; (ii) moderate to low metamorphic pressures; and (iii) the southward decrease in metamorphic pressures and temperatures.

Using thermal modelling, Barton & Hanson (1989) demonstrated that regional low-*P* metamorphism only occurs in areas with a large fraction of relatively evenly distributed igneous intrusions—otherwise sufficient heat is not available at shallow depths. It is possible that regional

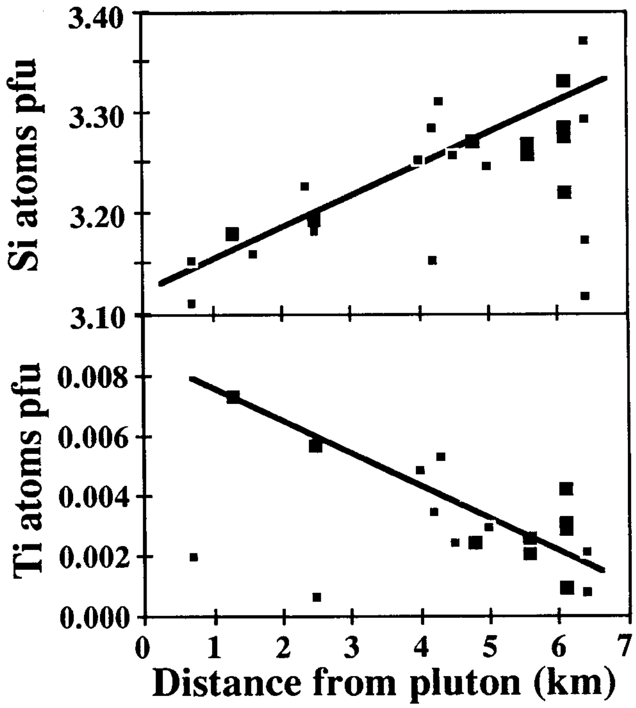

Fig. 11. Relationship between maximum Si and Ti contents (atoms per 11 oxygens) of phengites and proximity to the English Peak and Russian Peak calc-alkaline plutons. Phengites that coexist with microcline + quartz + chlorite ± biotite are shown with larger symbols.

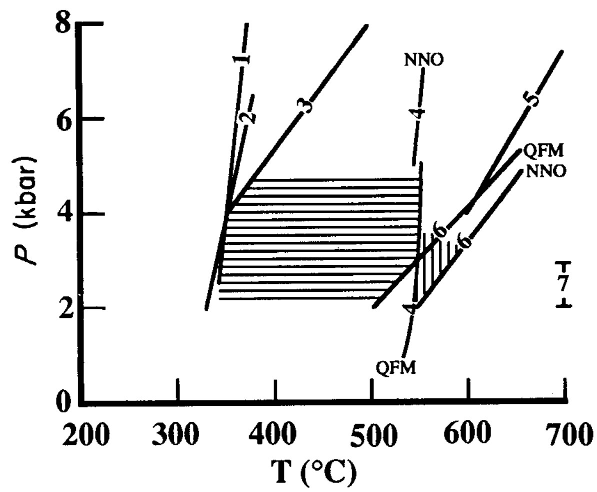

Fig. 12. *P–T* conditions for regional (horizontal lines) and contact (vertical lines) metamorphism of the metavolcanic rocks. Reactions indicated are: (1) pumpellyite + chlorite + quartz = clinozoisite + tremolite + H_2O (Liou *et al.*, 1985); (2) pumpellyite + chlorite + quartz = epidote + actinolite + H_2O (Nitsch, 1971); (3) maximum glaucophane stability (Maresch, 1977); (4) actinolitic hornblende + epidote + chlorite = tschermakitic hornblende + epidote (Liou *et al.*, 1974; Apted & Liou, 1983); (5) albite + epidote = plagioclase (Apted & Liou, 1983); and (6) epidote + quartz = grossular + anorthite + magnetite (Liou, 1973; Apted & Liou, 1983). QFM: quartz–fayalite–magnetite–H_2O buffer, NNO: nickel–nickel oxide–H_2O buffer. Also shown is (7) the pressure bracket inferred for crystallization of hornblende crystals in the English Peak pluton (see text).

metamorphism in the Sawyers Bar area, which pre-dated contact metamorphism, was caused by heat advected to shallow crustal levels by plutons like those that caused the contact metamorphism. The regional and contact metamorphism may thus be genetically linked, and nearly coeval. Heat for both events may have come from the same volcano-plutonic edifice that erupted the volcanic rocks. As a less likely alternative, the volcanism, regional metamorphism, contact metamorphism, and pluton emplacement may be unrelated. These possibilities might be differentiated by obtaining radiometric ages on igneous and metamorphic minerals, and by obtaining better constraints on the pressures during regional metamorphism.

Phengites near plutons contain more TiO_2 and less SiO_2 than those that grew during the regional metamorphism (Fig. 11). The magnitude of the SiO_2 decrease toward the plutons has implications for barometric estimations involving phengite. For example, Massone & Schreyer (1978) used the results of unreversed experiments in the

Table 2. Barometry of contact metamorphic rocks.

	Muscovite					Chlorite				Biotite				
	Si	Al	Fe	Mg	K	Si	Al	Fe	Mg	Si	Al	Fe	Mg	K
91M	3.11	2.70	0.09	0.10	0.93	2.88	2.49	1.19	3.42	2.85	1.59	0.81	1.67	0.91
351M	3.19	2.66	0.05	0.10	0.84	2.80	2.47	1.28	3.37	2.88	1.51	0.78	1.72	0.95

	Powell & Evans (1983)		Bucher-Nurminen (1987)		Massone & Schreyer (1987)
	ln (K_d)	P (kbar)	$\log_{10}$ (K_d)	P (kbar)	P (kbar)
91M	10.2	2–3	4.6	1–2	<1.5–2.5
351M	10.2	2–3	4.5	1–2	4–5

Both samples contain the assemblage muscovite + biotite + chlorite + quartz; 351M also contains microcline. Pressures are calculated for temperatures of 400–500° C, from figs 1 & 2 of Powell & Evans (1983), figs 1 & 2 of Bucher-Nurminen (1987), and fig. 3 of Massone & Schreyer (1987). Muscovite and biotite compositions are given as cations per 11 oxygens; chlorite composition as cations per 14 oxygens.

K_2O–MgO–Al_2O_3–SiO_2–H_2O (KMASH) system conducted in the temperature range 350–600° C to quantify changes in the Si content of phengite coexisting with biotite, quartz, and potassium feldspar, as a function of pressure and temperature. Two brackets for this same reaction were previously obtained by Velde (1965). Discrepancies between the two data sets prompted additional reformulations of this barometer by Powell & Evans (1983) using Velde's data, and by Bucher-Nurminen (1987) using Massone & Schreyer's data. For one sample containing muscovite + biotite + chlorite + quartz + microcline, we calculate contact metamorphic pressures of 1–2, 2–3, and 4–5 kbar, for Bucher-Nurminen's (1987), Powell & Evans' (1983) and Massone & Schreyer's (1987) formulations, respectively. For one sample containing muscovite + biotite + chlorite + quartz, Bucher-Nurminen's (1987) and Powell & Evans' (1983) formulations yield contact metamorphic pressures of 1–2 and 2–3 kbar, respectively. Because the crystallization pressure calculated for the English Peak pluton is 2–2.9 ± 0.5 kbar, we prefer the contact metamorphic pressures calculated from Bucher-Nurminen's (1987) and Powell & Evans' (1983) calibrations (Table 2).

CONCLUSIONS

Highly magnesian volcanic rocks in the Sawyers Bar area of the Klamath Mountains show metasomatic and textural effects of submarine metamorphism, regional metamorphism, and contact metamorphism following igneous crystallization. In general, the 'komatiitic' major-element affinities are incompatible with trace-element concentrations, which indicate eruption as oceanic intraplate, mildly alkalic basalts and immature arc tholeiites (Ernst *et al.*, 1991). The metavolcanic rocks are enriched in MgO (as much as 6 wt%) and depleted in Al_2O_3 and Na_2O relative to worldwide volcanic rocks. Correlation of 'excess' MgO with the volume per cent of hornblende (±clinopyroxene) suggests that the presence of cumulus phases may have produced much of the magnesian signature.

Substantial, relatively low-T submarine fluid–rock interaction caused enrichment of $\delta^{18}O$ from probable igneous values of *c.* 6‰ to *c.* 10‰. Bulk compositional shifts (e.g. Al_2O_3, Na_2O, and K_2O) may have occurred during submarine metamorphism as well.

Subsequent regional metamorphism (probably the mid-Jurassic Siskiyou event of Coleman *et al.*, 1988) appears to have involved little chemical exchange. Regional metamorphic grade decreases from greenschist facies (350–550° C, *c.* 3 kbar) southward to prehnite–actinolite facies (200–400° C, ≤3 kbar). The greenschist facies assemblages are actinolitic hornblende + biotite (only in Ti-rich rocks) + phengite + epidote + sodic plagioclase + microcline + chlorite + titanite + hematite + quartz. Less intensely recrystallized metabasaltic rocks in the south carry actinolite and prehnite. The moderate to low pressures of regional metamorphism are compatible with metamorphism in a magmatic arc and may be related to the heat sources causing eruption of the volcanic rocks.

Contact metamorphism at *c.* 2–2.9 kbar and at peak temperatures of *c.* 600° C around the English Peak and Russian Peak plutons produced 3–4-km-wide aureoles containing predominantly magnesio-hornblende + oligoclase + epidote + titanite + quartz. Igneous intrusion also increased $\delta^{18}O$ rock values by an additional 5‰ within 3–4 km of plutons, probably by exchange with intercalated metasedimentary rocks. The regional metamorphism may have been caused by heat advected to shallow crustal levels by plutons like those that caused the contact metamorphism.

ACKNOWLEDGEMENTS

This research was supported by the University of California, Los Angeles, by Stanford University and by the Department of Energy through grant DE-FG03-87ER13806 to W.G.E. Thanks are due to UCLA colleagues R. Jones for microprobe assistance and R. Alkaly for polished sections. We also thank R. E. Bevins, M. Cho, H. Day, J. Schumacher, G. Sen, and F. Spear for helpful reviews. The stable isotope analyses were supported by a grant from the Petroleum Research Fund of the American Chemical Society to M.D.B.

REFERENCES

Alt, J. C., Honnorez, J., Laverne, C. & Emmermann, R., 1986. Hydrothermal alteration of a 1 km section through the upper oceanic crust, Deep Sea Drilling Project hole 504B: mineralogy, chemistry, and evolution of seawater-basalt interactions. *Journal of Geophysical Research,* **91,** 10,309–10,355.

Ando, C. J., Irwin, W. P., Jones, D. L. & Saleeby, J. B., 1983. The ophiolitic North Fork terrane in the Salmon River region, central Klamath Mountains, California. *Geological Society of America Bulletin,* **94,** 236–252.

Apted, M. J. & Liou, J. G., 1983. Phase relations among greenschist, epidote–amphibolite, and amphibolite in a basaltic system. *American Journal of Science,* **283-A,** 328–354 (Orville volume).

Arndt, N. T. & Nesbitt, R. W., 1982a. Geochemistry of Munro Township basalts. In: *Komatiites* (eds Arndt, N. T. & Nisbet, E. G.), pp. 309–329. George Allen & Unwin, London.

Arndt, N. T. & Nisbet, E. G., 1982b. What is a komatiite? In: *Komatiites* (eds Arndt, N. T. & Nisbet, E. G.), pp. 19–28. George Allen & Unwin, London.

Barton, M. D. & Hanson, R. B., 1989. Magmatism and the development of low-pressure metamorphic belts: implications from the western United States and thermal modeling. *Geological Society of America Bulletin,* **101,** 1051–1065.

Beaty, D. W. & Taylor, H. P., Jr, 1982. The oxygen isotope geochemistry of komatiites: evidence for water–rock interaction. In: *Komatiites* (eds Arndt, N. T. & Nisbet, E. G.), pp. 267–280. George Allen & Unwin, London.

Blome, C. D. & Irwin, W. P., 1983. Tectonic significance of Late Paleozoic to Jurassic radiolarians from the North Fork terrane, Klamath Mountains, California. In: *Pre-Jurassic Rocks in Western North American Suspect Terranes* (ed. Stevens, C.H.), pp. 77–87. Pacific Section of Economic Paleontologists and Mineralogists, Los Angeles, California.

Bothwick, J. & Harmon, R. S., 1982. A note regarding ClF_3 as an alternative to BrF_5 for oxygen isotope analysis. *Geochimica et Cosmochimica Acta,* **46,** 1665–1668.

Bowers, T. S. & Taylor, H. P., Jr, 1985. An integrated chemical and stable isotope model of the origin of midocean ridge hot spring systems. *Journal of Geophysical Research*, **90**, 12,583–12,606.

Bucher-Nurminen, K., 1987. A recalibration of the chlorite–biotite–muscovite geobarometer. *Contributions to Mineralogy and Petrology*, **96**, 519–522.

Cameron, W. E. & Nisbet, E. G., 1982. Phanerozoic analogues of komatiitic basalts. In: *Komatiites* (eds Arndt, N. T. & Nisbet, E. G.), pp. 29–49. George Allen & Unwin, London.

Coleman, R. G., Manning, C. E., Mortimer, N., Donato, M. M. & Hill, L. B. 1988. Tectonic and regional metamorphic framework of the Klamath Mountains and adjacent Coast Ranges, California and Oregon. In: *Metamorphism and Crustal Evolution of the Western United States* (ed. Ernst, W. G.) Rubey Vol. VII, p. 1061–1096. Prentice Hall, Englewood Cliffs, NJ.

Criss, R. E. & Taylor, H. P., Jr, 1986. Meteoric–hydrothermal systems. In: *Stable Isotopes in High Temperature Geologic Processes, Reviews in Mineralogy*, Vol. 16 (eds Valley, J. W., Taylor, Jr. H. P., & O'Neil, J. R.), pp. 373–424.

Donato, M. M., 1989. Metamorphism of an ophiolitic tectonic mélange, northern California Klamath Mountains, USA. *Journal of Metamorphic Geology*, **7**, 515–528.

Ernst, W. G., 1987. Mafic meta-igneous arc rocks of apparent komatiitic affinities, Sawyers Bar area, central Klamath Mountains, northern California. *Special Publication of the Geochemical Society*, **1**, 191–208.

Ernst, W. G., 1990. Accretionary terrane in the Sawyers Bar area of the Western Triassic and Paleozoic belt, central Klamath Mountains, northern California. *Geological Society of America Special Paper*, **255**, 297–306.

Ernst, W. G., Hacker, B. R., Barton, M. D. & Sen, G., 1991. Occurrence, geochemistry and igneous petrogenesis of magnesian metavolcanic rocks from the WTrPz belt, central Klamath Mountains, northern California. *Geological Society of America Bulletin*, **103**, 56–72.

Goodge, J. W., 1989. Evolving early Mesozoic convergent margin deformation, central Klamath Mountains, northern California. *Tectonics*, **8**, 845–864.

Hacker, B. R. & Ernst, W. G., 1991. Permian to Jurassic tectonic evolution of the Hayfork, Salmon River, North Fork, and Stuart Fork terranes, Klamath Mountains. *Geological Society of America Abstracts with Programs*, **23**, 32.

Hill, L. B., 1985. Metamorphic, deformational and temporal constraints on terrane assembly, northern Klamath Mountains, California. In: *Tectonostratigraphic Terranes of the Circum-Pacific Region* (ed. Howell, D. G.), Earth Science Series, Vol. 1, pp. 173–186. Circum-Pacific Council for Energy & Mineral Resources, Houston, TX.

Hoefs, J., 1987. *Stable Isotope Geochemistry*. Springer-Verlag, Berlin, 241 pp.

Hollister, L. S., Grissom, G. C., Peters, E. K., Stowell, H. H. & Sisson, V. B., 1987. Confirmation of the empirical correlation of Al in hornblende with pressure of solidification of calc-alkaline plutons. *American Mineralogist*, **72**, 231–239.

Hynes, A., 1982. A comparison of amphiboles from medium- and low-pressure metabasites. *Contributions to Mineralogy and Petrology*, **81**, 119–125.

Johnson, M. C. & Rutherford, M. J., 1989. Experimental calibration of the aluminium-in-hornblende geobarometer with application to Long Valley caldera (California) volcanic rocks. *Geology*, **17**, 837–841.

Laird, J. & Albee, A. L., 1981a. High-pressure metamorphism in mafic schist from northern Vermont. *American Journal of Science*, **281**, 97–126.

Laird, J. & Albee, A. L., 1981b. Pressure, temperature, and time indicators in mafic schist: their application to reconstructing the polymetamorphic history of Vermont. *American Journal of Science*, **281**, 127–175.

Laird, J., Lanphere, M. A. & Albee, A. L., 1984. Distribution of Ordovician and Devonian metamorphism in mafic and pelitic schists from northern Vermont. *American Journal of Science*, **284**, 376–413.

Liou, J. G., 1973. Synthesis and stability relations of epidote, $Ca_2Al_2FeSi_3O_{12}(OH)$. *Journal of Petrology*, **14**, 381–413.

Liou, J. G., Kuniyoshi, S. & Ito, K., 1974. Experimental studies of the phase relations between greenschist and amphibolite in a basaltic system. *American Journal of Science*, **274**, 613–632.

Liou, J. G., Maruyama, S. & Cho, M., 1985. Phase equilibria and mineral parageneses of metabasites in low-grade metamorphism. *Mineralogical Magazine*, **49**, 321–333.

Liou, J. G., Maruyama, S. & Cho, M., 1987. Very low-grade metamorphism of volcanic and volcaniclastic rocks—mineral assemblages and mineral facies. In: *Low Temperature Metamorphism* (ed. Frey, M.), pp. 59–112. Blackie, Glasgow.

Maresch, W. V., 1977. Experimental studies on glaucophane: an analysis of present knowledge. *Tectonophysics*, **43**, 109–125.

Maruyama, S., Liou, J. G. & Suzuki, K., 1982. The peristerite gap in low-grade metamorphic rocks. *Contributions to Mineralogy and Petrology*, **81**, 268–276.

Massone, H.-J. & Schreyer, W. 1987. Phengite geobarometry based on the limiting assemblage with K-feldspar, phlogopite, and quartz. *Contributions to Mineralogy and Petrology*, **96**, 212–224.

Miyashiro, A., 1973. *Metamorphism and Metamorphic Belts*. George Allen & Unwin, London, 492 pp.

Muehlenbachs, K., 1986. Alteration of the oceanic crust and the ^{18}O history of seawater. In: *Stable Isotopes in High Temperature Geologic Processes* (eds Valley, J. W., Taylor, H. P. & O'Neil, J. R.), *Reviews in Mineralogy*, Vol. 16, pp. 425–444.

Nitsch, K.-H., 1971. Stabilitätsbeziehungen von Prehnite-und Pumpellyite-haltigen Paragenesen. *Contributions to Mineralogy and Petrology*, **30**, 240–260.

Powell, R. & Evans, J. A., 1983. A new geobarometer for the assemblage biotite–muscovite–chlorite–quartz. *Journal of Metamorphic Geology*, **1**, 331–336.

Rock, N. M. S. & Leake, B. E., 1984. The International Mineralogical Association amphibole nomenclature scheme: computerization and its consequences. *Mineralogical Magazine*, **48**, 211–227.

Seyfried, W. E., Jr, Berndt, M. E. & Seewald, J. S., 1988. Hydrothermal alteration processes at mid-ocean ridges: constraints from diabase alteration experiments, hot-spring fluids, and composition of the oceanic crust. *Canadian Mineralogist*, **26**, 787–804.

Silberling, N. J., Jones, D. L., Blake, M. C., Jr & Howell, D. G., 1987. Lithotectonic terrane map of the western conterminous United States. *Miscellaneous Field Studies Map MF-1874-C, scale 1:2,500,000.*

Taylor, H. P., Jr, 1968. The ^{18}O geochemistry of igneous rocks. *Contributions to Mineralogy and Petrology*, **19**, 1–71.

Velde, B., 1965, Phengite micas: synthesis, stability, and natural occurrence. *American Journal of Science*, **263**, 886–913.

Wright, J. E. & Fahan, M. R., 1988. An expanded view of Jurassic orogenesis in the western United States Cordillera: Middle Jurassic (pre-Nevadan) regional metamorphism and thrust faulting within an active arc environment, Klamath Mountains, California. *Geological Society of America Bulletin*, **100**, 859–876.

Yoshiasa, A. & Matsumoto, T., 1985. Crystal structure refinement and crystal chemistry of pumpellyite. *American Mineralogist*, **70**, 1011–1019.

Received 7 April 1990; revision accepted 27 April 1991.